

Anisotropic magnetothermopower: Contribution of interband relaxation

J.-E. Wegrowe, Q. Anh Nguyen, M. Al-Barkhi, J.-F. Dayen, T. L. Wade, and H.-J. Drouhin
*Laboratoire des Solides Irradiés, Ecole Polytechnique, CNRS-UMR 7642 and CEA/DSM/DRECAM/CAPMAG,
 91128 Palaiseau Cedex, France*

(Received 18 October 2005; published 25 April 2006)

Spin injection in metallic normal/ferromagnetic junctions is investigated taking into account interband relaxation and the consequences in terms of thermoelectric power. On the basis of a generalized two-channel model, it is shown that there is an interface resistance and thermoelectric power contribution due to anisotropic scattering, besides spin accumulation and giant magnetoresistance. The corresponding expression of the thermoelectric power is derived and compared with the expression accounting for the thermoelectric power produced by the giant magnetoresistance. Measurements of anisotropic magnetothermoelectric power are presented in electrodeposited Ni nanowires contacted with Ni, Au, and Cu. It is shown that a thermoelectric power is generated at the interfaces of the nanowire and that the experimental results strongly support the model.

DOI: [10.1103/PhysRevB.73.134422](https://doi.org/10.1103/PhysRevB.73.134422)

PACS number(s): 75.47.De, 72.25.Hg

I. INTRODUCTION

In order to explain the high resistance and high thermoelectric power observed in transition metals, Mott introduced the concept of spin-polarized current and suggested that s - d interband scattering plays an essential role in the conduction properties.¹ This approach, in terms of two conduction bands, explained the existence of a spin-polarized current in the $3d$ ferromagnetic materials and was used for the description of anisotropic magnetoresistance^{2,3} (AMR) and thermoelectric power.^{4,5} With the discovery of giant magnetoresistance⁶ (GMR) and related effects, a development of spintronics focused a discussion of spin-flip scattering occurring between spin-polarized conducting channels. The two-channel model, which describes the conduction electrons with majority and minority spins, is applied with great efficiency to GMR and spin injection effects,⁷⁻¹¹ including metal/semiconductor¹² and metal/supraconductor interfaces.¹³ In this context, it is sufficient to describe the diffusion process in terms of spin-flip scattering without the need to invoke interband s - d scattering.

Magnetothermoelectric power (MTEP) experiments in GMR structures,¹⁴⁻²⁰ however, point out the need for a deeper understanding of the dissipative mechanism responsible for the giant magnetothermopower related to GMR. The problem of s - d electronic relaxation at the interface was also put forward in the context of current-induced magnetization reversal mechanisms in various systems exhibiting AMR.²¹⁻²⁵ However, the interface contribution to the resistance in relation to AMR has so far not been investigated. The aim of the present work is to study the nonequilibrium contribution of a normal/ferromagnetic (N/F) interface to both the resistance and thermoelectric power.

For our purpose, it is convenient to generalize the two-spin-channel approach to any relevant transport channels—i.e., to any distinguishable electron populations α and γ .²⁶ The local out-of-equilibrium state near the junction is then described by a nonvanishing chemical-potential difference between these two populations: $\Delta\mu_{\alpha\gamma} = \mu_{\alpha} - \mu_{\gamma} \neq 0$.¹¹ Corollarily, assuming that the presence of a junction induces a deviation from the local equilibrium, the α and γ populations

can be defined by the $\alpha \rightarrow \gamma$ relaxation mechanism itself, which allows the local equilibrium to be recovered in the bulk material [$\lim_{z \rightarrow \pm\infty} \Delta\mu(z) = 0$]. In this context,^{11,25} the basic idea we develop here is that, beyond spin-flip relaxation, interband s - d relaxation also plays a crucial role in the interface magnetoresistance of magnetic nanostructures. Though similar ideas have been suggested in previous spintronics studies,^{1-3,18,27,28} the originality of this work is to deal with interband relaxation on an equal footing with spin-flip relaxation²⁵ in the framework of a *thermokinetic approach*. For this purpose, the two-spin-channel model is generalized, with the introduction of the corresponding transport coefficients: the conductivities σ_{α} and σ_{γ} of each channel define the total conductivity $\sigma_t = \sigma_{\alpha} + \sigma_{\gamma}$ and the conductivity asymmetry $\beta = (\sigma_{\alpha} - \sigma_{\gamma}) / \sigma_t$; the relaxation between both channels is described by the parameter L (or, equivalently, the relevant relaxation times $\tau_{\gamma \rightarrow \alpha}$). It is shown that this two-channel model can be applied straightforwardly to the description of MTEP by introducing an extra transport parameter which is nothing but the derivative of β with respect to the energy. The predictions of the model are compared with experimental results of anisotropic MTEP measured in electrodeposited nanowires.

The article is structured as follows: General expressions of the interface contributions of resistance (Sec. II) and thermoelectric power (Sec. III) are derived and applied to the case of AMR and GMR systems (Sec. IV) and to the corresponding MTEP (Sec. V). It is shown that a contribution of the interface resistance related to AMR and the corresponding MTEP should be expected. The experimental study performed on single-contacted Ni nanowires (Sec. VI) confirms the presence of an anisotropic MTEP, which is produced by the interfaces.

II. OUT-OF-EQUILIBRIUM RESISTANCE

In the framework of the two-conducting-channel model, which includes relaxation from one channel to the other, it is possible to show, on the basis of the entropy variation,¹¹ that the kinetics is described by the following Onsager equations:

$$J_\alpha = -\frac{\sigma_\alpha}{e} \frac{\partial \mu_\alpha}{\partial z}, \quad J_\gamma = -\frac{\sigma_\gamma}{e} \frac{\partial \mu_\gamma}{\partial z},$$

$$\dot{\Psi}_{\alpha\gamma} = L(\mu_\alpha - \mu_\gamma), \quad (1)$$

where $\dot{\Psi}_{\alpha\gamma}$ describes the relaxation from the channel α to the other channel γ in terms of the velocity of the reaction $\alpha \rightarrow \gamma$. The Onsager coefficient L is inversely proportional to the relaxation times $\tau_{\alpha \leftrightarrow \gamma}$:

$$L \propto \left(\frac{f}{\tau_{\alpha \rightarrow \gamma}} + \frac{g}{\tau_{\gamma \rightarrow \alpha}} \right), \quad (2)$$

where f and g account for the electric charge distribution and are close to unity. The out-of-equilibrium configuration is quantified by the chemical affinity $\Delta\mu = \mu_\alpha - \mu_\gamma$ —i.e., the chemical potential difference of the reaction.

Furthermore, in the case of a stationary regime, the conservation laws lead to

$$\frac{dn_\alpha}{dt} = -\frac{\partial J_\alpha}{\partial z} - \dot{\Psi}_{\alpha\gamma} = 0,$$

$$\frac{dn_\gamma}{dt} = -\frac{\partial J_\gamma}{\partial z} + \dot{\Psi}_{\alpha\gamma} = 0, \quad (3)$$

where n_α , n_γ are the densities of particles in each channel. The total current J_t is constant:

$$J_t = J_\alpha + J_\gamma = -\frac{1}{e} \frac{\partial}{\partial z} (\sigma_\alpha \mu_\alpha + \sigma_\gamma \mu_\gamma). \quad (4)$$

The expression of Ohm's law, $J_t = -\sigma_t \partial\Phi/\partial z$, is recovered by introducing the measured electric potential Φ and the total conductivity $\sigma_t = \sigma_\alpha + \sigma_\gamma$ (Ref. 29):

$$e\Phi = \frac{1}{\sigma_t} (\sigma_\alpha \mu_\alpha + \sigma_\gamma \mu_\gamma). \quad (5)$$

Let us assume that the two channels collapse to a unique conduction channel for a specific configuration, the reference, which is a local equilibrium situation: $\Delta\mu_{eq} = 0$. The out-of-equilibrium contribution to the resistance, R^{ne} , is calculated through the relation

$$J_t e R^{ne} = \int_A^B \frac{\partial}{\partial z} [\mu_\alpha - e\Phi(z)] dz = \int_A^B \frac{\partial}{\partial z} [\mu_\gamma - e\Phi(z)] dz, \quad (6)$$

so that

$$R^{ne} = -\frac{1}{J_t e} \int_A^B \frac{\sigma_\alpha - \sigma_\gamma}{2\sigma_t} \frac{\partial \Delta\mu}{\partial z} dz, \quad (7)$$

where the measurement points A and B are located far enough from the interface (inside the bulk) so that $\Delta\mu(A) = \Delta\mu(B) = 0$ (see Fig. 1). The integral in Eqs. (6) is performed over the regular part of the function only (Φ and $\sigma_{\alpha\gamma}$ are discontinuous).³⁰ Equation (7) allows the out-of-equilibrium resistance at a simple junction between two layers (composed by the layers I and II) to be easily calculated. If the

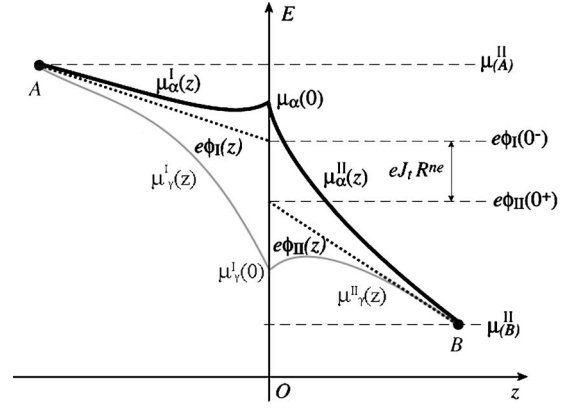


FIG. 1. Chemical potential profile over the interval $[A, B]$ in the α and γ channels. The A and B points verify $\mu_\alpha(A) = \mu_\gamma(A)$ and $\mu_\alpha(B) = \mu_\gamma(B)$. The two straight lines represent the Φ variation in each region (Φ_I, Φ_{II}). It can be directly seen that the out-of-equilibrium resistance R^{ne} is determined by the Φ discontinuity at the interface.

junction is set at $z=0$ and the conductivities are, respectively, σ_i^I and σ_i^{II} ($i = \{\alpha, \gamma\}$), we have

$$J_t e R^{ne} = \int_A^0 \frac{\sigma_\alpha^I - \sigma_\gamma^I}{2\sigma_t^I} \frac{\partial \Delta\mu^I}{\partial z} dz + \int_0^B \frac{\sigma_\alpha^{II} - \sigma_\gamma^{II}}{2\sigma_t^{II}} \frac{\partial \Delta\mu^{II}}{\partial z} dz. \quad (8)$$

The equilibrium is recovered in the bulk, so that

$$R^{ne} = \left(\frac{\sigma_\alpha^I - \sigma_\gamma^I}{\sigma_t^I} - \frac{\sigma_\alpha^{II} - \sigma_\gamma^{II}}{\sigma_t^{II}} \right) \frac{\Delta\mu(0)}{2J_t e}. \quad (9)$$

The chemical potential difference $\Delta\mu(z)$, which accounts for the pumping force opposed to the relaxation $\alpha \rightarrow \gamma$, is obtained by solving the diffusion equation deduced from Eqs. (1) and (3) (Refs. 7–11):

$$\frac{\partial^2 \Delta\mu(z)}{\partial z^2} = \frac{\Delta\mu(z)}{l_{diff}^2}, \quad (10)$$

where

$$l_{diff}^{-2} = eL(\sigma_\alpha^{-1} + \sigma_\gamma^{-1}) \quad (11)$$

is the diffusion length related to the $\alpha \rightarrow \gamma$ relaxation.

At the interface ($z=0$), the continuity of the currents for each channel is written: $J_\alpha^I(0) = J_\alpha^{II}(0)$, where

$$J_\alpha(0) = -\frac{\sigma_\alpha \sigma_\gamma}{e \sigma_t} \frac{\partial \Delta\mu}{\partial z} + \frac{\sigma_\alpha}{\sigma_t} J_t, \quad (12)$$

which leads to the general relation

$$\Delta\mu(0) = \left(\frac{\sigma_\alpha^I}{\sigma_t^I} - \frac{\sigma_\alpha^{II}}{\sigma_t^{II}} \right) \left(\frac{\sigma_\alpha^I \sigma_\gamma^I}{\sigma_t^I l_{diff}^I} + \frac{\sigma_\alpha^{II} \sigma_\gamma^{II}}{\sigma_t^{II} l_{diff}^{II}} \right)^{-1} e J_t. \quad (13)$$

Inserting Eq. (13) into Eq. (9), we obtain the general expression for the out-of-equilibrium resistance (per unit area) produced by the $\alpha \rightarrow \gamma$ relaxation mechanism at a junction:

$$R^{ne} = \left(\frac{\sigma_\alpha^J - \sigma_\gamma^J}{2\sigma_t^J} - \frac{\sigma_\alpha^{II} - \sigma_\gamma^{II}}{2\sigma_t^{II}} \right) \left(\frac{\sigma_\alpha^J}{\sigma_t^J} - \frac{\sigma_\alpha^{II}}{\sigma_t^{II}} \right) \times \left(\sqrt{\frac{\sigma_\alpha^J \sigma_\gamma^J eL^J}{\sigma_t^J}} + \sqrt{\frac{\sigma_\alpha^{II} \sigma_\gamma^{II} eL^{II}}{\sigma_t^{II}}} \right)^{-1}. \quad (14)$$

It is convenient to describe the conductivity asymmetry by a parameter β such that $\sigma_\alpha = \sigma_t(1+\beta)/2$ and $\sigma_\gamma = \sigma_t(1-\beta)/2$. The out-of-equilibrium contribution to the resistance then takes the following form:

$$R^{ne} = \frac{1}{2} \frac{(\beta_I - \beta_{II})^2}{\sqrt{eL^J \sigma_t^J (1 - \beta_I^2)} + \sqrt{eL^{II} \sigma_t^{II} (1 - \beta_{II}^2)}}, \quad (15)$$

where we have used the relation

$$l_{diff}^{-1} = 2 \sqrt{\frac{eL}{\sigma_t(1 - \beta^2)}}. \quad (16)$$

III. GIANT MAGNETORESISTANCE VS ANISOTROPIC MAGNETORESISTANCE

A. Giant magnetoresistance

The most famous example of interface out-of-equilibrium resistance described in the preceding section is the giant magnetoresistance⁶ occurring near a junction composed of two ferromagnetic layers F_1/F_2 made out of the same metal. The electronic populations are the spin-polarized carriers quantized along the ferromagnetic order parameter $\alpha = \uparrow, \gamma = \downarrow$. The diffusion length is the spin-diffusion length $l_{diff} = l_{sf}$. The $\alpha \rightarrow \gamma$ relaxation is the spin-flip relaxation and tends to balance the deviation from the local equilibrium. This process leads to a spin accumulation described by the generalized force $\Delta\mu = \mu_\uparrow - \mu_\downarrow$. The local equilibrium ($\Delta\mu = 0$) is recovered in the bulk ferromagnet at the voltage probes or, equivalently, in the case of two parallel magnetic configurations. When the magnetization of the two layers are parallel, we have, indeed, $\sigma_\uparrow^J = \sigma_\uparrow^{II}$ and $\sigma_\downarrow^J = \sigma_\downarrow^{II}$, and $R^{ne} = 0$. In contrast, for an antiparallel configuration $\sigma_\uparrow^J = \sigma_\downarrow^{II}$ and $\sigma_\downarrow^J = \sigma_\uparrow^{II}$. In terms of conductivity asymmetry β_s , we have $\sigma_\uparrow = \sigma_t(1+\beta_s)/2$ and $\sigma_\downarrow = \sigma_t(1-\beta_s)/2$ (the subscript s refers to the s type—possibly sd -hybridized—conduction band). The out-of-equilibrium resistance is written

$$R_{GMR}^{\uparrow\downarrow} = \frac{\beta_s^2}{\sigma_t(1 - \beta_s^2)} l_{sf} = \frac{\beta_s^2}{\sqrt{eL\sigma_t(1 - \beta_s^2)}}. \quad (17)$$

This expression is the well-known giant magnetoresistance^{7-11,31,32} measured in various $F_1/N/F_2$ devices. It is usually presented as the normalized ratio

$$\frac{R_{GMR}^{\uparrow\downarrow}}{R_0} = \frac{\beta_s^2 l_{sf}}{1 - \beta_s^2 \Lambda} \quad (18)$$

measured on a layer of thickness Λ , where $R_0 = R^{\uparrow\uparrow} = R^{\downarrow\downarrow} = \Lambda/\sigma_t$ is the overall resistance of the layers (also per surface units).

In the case of a single N/F junction, we have $\sigma_\alpha^J = \sigma_\gamma^J$ in the normal metal and $\sigma_\alpha^{II} \neq \sigma_\gamma^{II}$ in the ferromagnetic metal. The out-of-equilibrium resistance is written

$$R_{GMR}^{N-F} = \frac{1}{2} \frac{\beta_s^2}{\sqrt{eL^N \sigma_t^N} + \sqrt{eL^F \sigma_t^F (1 - \beta_s^2)}}. \quad (19)$$

This is the out-of-equilibrium resistance arising in a single magnetic layer. It is worth pointing out that, in spite of the existence of spin accumulation and nonvanishing out-of-equilibrium resistance, it is not possible to measure a deviation of R_{GMR}^{N-F} from a reference state because the resistance does not vary with the magnetic configurations or with any well-controlled external parameters (except in the case of domain wall scattering, discussed, e.g., in Ref. 33). In other words, R_{GMR} is present but there is nevertheless no analyzer, or probe, to detect it. Although the GMR results are well known, the more general equation (14) allows one to push the discussion about nonequilibrium resistances beyond GMR effects.

B. Interface magnetoresistance

From our generalized approach one should predict the existence of a *nonequilibrium anisotropic magnetoresistance* (NEAMR) due to the interface. The anisotropic magnetoresistance (AMR) is characterized by a conductivity $\sigma_i(\theta)$ which depends on the angle $\theta = (\vec{I}, \vec{M})$ between the *direction of the current* and the *magnetization*. In single-domain structures, the angle θ is tuned with the applied magnetic field which modifies the magnetization direction. In contrast to GMR ($\uparrow \downarrow$ relaxation), AMR is a bulk effect that necessarily involves at least one anisotropic relaxation channel $\alpha \rightarrow \gamma(\theta)$ which is controlled by the direction of the magnetization (and is hence related to spin-orbit coupling).³ Although generated by spin-dependent electronic relaxations, the $\alpha \rightarrow \gamma(\theta)$ relaxation channel does not necessarily involve spin-flip scattering. It is generally assumed that *the relaxation from the isotropic s minority channel $\alpha = s\downarrow$ to the anisotropic d minority channels $\gamma = d\downarrow$ is the main contribution to AMR in 3d ferromagnets*.^{1-3,25,34} In the *normal metal* (here normal means with no d -band effect), the conductivity of the (minority) d channel is vanishing, so that $\beta_{sd}^N = 1$. The out-of-equilibrium magnetoresistance is then a function of $\theta(\vec{M})$ defined by

$$R_{AMR}^{N-F}(\theta) = \frac{1}{2} \frac{[1 - \beta_{sd}(\theta)]^2}{\sqrt{eL_{sd}(\theta)\sigma_t(\theta)[1 - \beta_{sd}^2(\theta)]}}, \quad (20)$$

where $\beta_{sd}(\theta)$ is the conductivity asymmetry corresponding to the AMR relaxation channels; $\sigma_\alpha(\theta) = \sigma_t(\theta)[1 + \beta_{sd}(\theta)]/2$ and $\sigma_\gamma(\theta) = \sigma_t(\theta)[1 - \beta_{sd}(\theta)]/2$ in the ferromagnet. In terms of diffusion length and normalized to the bulk AMR $R_0(\theta)$, the NEAMR is written

$$\frac{R_{AMR}^{N-F}(\theta)}{R_0(\theta)} = \left(\frac{1 - \beta_{sd}(\theta)}{1 + \beta_{sd}(\theta)} \right) \frac{l_{diff}(\theta)}{\Lambda}, \quad (21)$$

where Λ is the layer thickness. However, the contribution of $R_{AMR}^{N-F}(\theta)$ is difficult to measure because l_{diff} is expected to be

small (nanometric or below) and the direct bulk contribution of the AMR dominates in usual configurations (see, however, Refs. 31 and 32 for a possible contribution in $F_1/N/F_2$ devices).

IV. OUT-OF-EQUILIBRIUM MAGNETOTHERMOPOWER

Since, in metallic structures, the heat transfer is carried by the conduction electrons, it is possible to study the electronic transport coefficients by performing thermoelectric power measurements while applying a temperature gradient to the sample. TEP is usually characterized through the bulk Seebeck coefficients, while imposing a temperature gradient under zero electric current (open circuit). In the same manner as for GMR, TEP is composed of a bulk contribution and an out-of-equilibrium contribution due to the interfaces (see Sec. IV B). Previous investigations of the interface contribution to the magnetothermoelectric power have been performed exclusively in GMR structures, with typical sizes of the magnetic layers below the spin-diffusion length (spin-valve structures).^{14–20} In this very case, the experimental results show that the spin-dependent thermopower is nearly proportional to the GMR. As will be shown below, the situation is similar in the case of single ferromagnetic layers exhibiting AMR.

In the following, the temperature gradient is assumed to be uniform: $\nabla T = \Delta T/\Lambda$, where Λ is the length of the wire and ΔT is the temperature difference between the two terminals. This simplifying assumption allows us to recover the diffusion equation (10). The Onsager relations follow by adding the heat flows $J_{\alpha\gamma}^Q$ of the two channels:

$$J_\alpha = -\frac{\sigma_\alpha}{e} \frac{\partial \mu_\alpha}{\partial z} + S_\alpha \sigma_\alpha \frac{\partial T}{\partial z},$$

$$J_\gamma = -\frac{\sigma_\gamma}{e} \frac{\partial \mu_\gamma}{\partial z} + S_\gamma \sigma_\gamma \frac{\partial T}{\partial z}, \quad J_\alpha^Q = \lambda_\alpha \frac{\partial T}{\partial z} - \frac{\pi_\alpha}{e} \frac{\partial \mu_\alpha}{\partial z},$$

$$J_\gamma^Q = \lambda_\gamma \frac{\partial T}{\partial z} - \frac{\pi_\gamma}{e} \frac{\partial \mu_\gamma}{\partial z}, \quad \Psi_{\alpha\gamma} = L(\mu_\alpha - \mu_\gamma), \quad (22)$$

where S_i and λ_i , $i=\{\alpha, \gamma\}$, are, respectively, the Seebeck and Fourier coefficients of each channel and π_i/σ_i is the Peltier coefficient.

Hereafter, we will not study the channel-dependent heat flow $J_{\alpha\gamma}^Q$. The thermopower is deduced from Eqs. (22) following step by step the method developed in the previous section and incorporating the condition $J_t=0$. In the bulk metal, the local equilibrium condition leads to the relation

$$J_t(\infty) = -\sigma_t \frac{\partial \Phi}{\partial z}(\infty) + S_t \sigma_t \frac{\Delta T}{\Lambda} = 0, \quad (23)$$

which yields

$$\frac{\partial \Phi}{\partial z}(\infty) = S_t \frac{\Delta T}{\Lambda}, \quad (24)$$

where

$$S_t = \frac{\sigma_\alpha S_\alpha + \sigma_\gamma S_\gamma}{\sigma_\alpha + \sigma_\gamma} \quad (25)$$

is the *reference thermopower* corresponding to the bulk, or the equilibrium TEP. The effective current (analogous to the total current in the GMR calculation) $J_{eff} = -S_t \sigma_t (\Delta T/\Lambda)$ is *different* in both sides of the junction (like the conductivity σ_t , the Seebeck coefficient S_t is discontinuous at the interface).

From Eqs. (22) and (12), the continuity of the currents $J_\alpha^I(0) = J_\alpha^{II}(0)$ leads to the following chemical-potential splitting at the interface:

$$\Delta \mu(0) = [\sigma_\alpha^I (S_\alpha^I - S_t^I) - \sigma_\alpha^{II} (S_\alpha^{II} - S_t^{II})] \times \left(\sqrt{\frac{\sigma_\alpha^I \sigma_\gamma^I e L^I}{\sigma_t^I}} + \sqrt{\frac{\sigma_\alpha^{II} \sigma_\gamma^{II} e L^{II}}{\sigma_t^{II}}} \right)^{-1} e \frac{\Delta T}{\Lambda}. \quad (26)$$

The chemical-potential splitting $\Delta \mu(0)$ is analogous to that calculated in Sec. II, Eq. (13), for the GMR, after introducing the effective current $J_{eff} = -S_t \sigma_t (\Delta T/\Lambda)$:

$$\Delta \mu(0) = e \left(J_{eff}^I \frac{S_\alpha^I - S_\gamma^I \sigma_\alpha^I \sigma_\gamma^I}{S_t^I \sigma_t^I} - J_{eff}^{II} \frac{S_\alpha^{II} - S_\gamma^{II} \sigma_\alpha^{II} \sigma_\gamma^{II}}{S_t^{II} \sigma_t^{II}} \right) \times \left(\sqrt{\frac{\sigma_\alpha^I \sigma_\gamma^I e L^I}{\sigma_t^I}} + \sqrt{\frac{\sigma_\alpha^{II} \sigma_\gamma^{II} e L^{II}}{\sigma_t^{II}}} \right)^{-1}. \quad (27)$$

Here again [see Eq. (7)], the out-of-equilibrium thermopower Σ^{ne} can be defined from the reference corresponding to local equilibrium condition, $\Delta \mu_{eq} = 0$ and $J_\alpha = J_\gamma = 0$:

$$\Sigma^{ne} \frac{\Delta T}{\Lambda} = \frac{1}{e} \int_A^B \left(\frac{\partial \mu_\alpha}{\partial z} - e \frac{\partial \Phi}{\partial z} \right) dz = \frac{1}{e} \int_A^B \left(\frac{\partial \mu_\alpha}{\partial z} - e S_t \frac{\partial T}{\partial z} \right) dz, \quad (28)$$

where A (B) is located in the layer I (II), at the distance Λ^I (Λ^{II}), far enough from the interface (inside the bulk). This is the same expression as that calculated for the out-of-equilibrium resistance in Eq. (9). We obtain

$$\Sigma^{ne} \frac{\Delta T}{\Lambda} = - \left(\frac{\sigma_\alpha^I - \sigma_\gamma^I}{\sigma_t^I} - \frac{\sigma_\alpha^{II} - \sigma_\gamma^{II}}{\sigma_t^{II}} \right) \frac{\Delta \mu(0)}{2e}. \quad (29)$$

Making use of Eq. (26) we deduce the out-of-equilibrium TEP:

$$\Sigma^{ne} = -\frac{1}{2} \left(\frac{\sigma_\alpha^I - \sigma_\gamma^I}{\sigma_t^I} - \frac{\sigma_\alpha^{II} - \sigma_\gamma^{II}}{\sigma_t^{II}} \right) \left(\frac{\sigma_\alpha^I \sigma_\gamma^I}{\sigma_t^I} (S_\alpha^I - S_\gamma^I) - \frac{\sigma_\alpha^{II} \sigma_\gamma^{II}}{\sigma_t^{II}} \right) \times (S_\alpha^{II} - S_\gamma^{II}) \left(\sqrt{\frac{\sigma_\alpha^I \sigma_\gamma^I e L^I}{\sigma_t^I}} + \sqrt{\frac{\sigma_\alpha^{II} \sigma_\gamma^{II} e L^{II}}{\sigma_t^{II}}} \right)^{-1}. \quad (30)$$

This is the general expression of the out-of-equilibrium MTEP. In the following, it will be expressed in terms of transport-coefficient asymmetry β . Let us define the parameters $S_+ = (S_\alpha + S_\gamma)/2$ and $S_- = (S_\alpha - S_\gamma)/2$. We see that $S_t = \frac{1}{2}[(1+\beta)S_\alpha + (1-\beta)S_\gamma]$, so that the overall Seebeck coefficient is rewritten:

$$S_t = S_+ + \beta S_-.$$

The out-of-equilibrium interface thermopower takes the form

$$\Sigma^{ne} = -(\beta^I - \beta^{II}) \frac{\sigma_t^I [1 - (\beta^I)^2] S_-^I - \sigma_t^{II} [1 - (\beta^{II})^2] S_-^{II}}{\sqrt{eL^I \sigma_t^I [1 - (\beta^I)^2]} + \sqrt{eL^{II} \sigma_t^{II} [1 - (\beta^{II})^2]}}. \quad (31)$$

It is possible to investigate further this relation by using the microscopic Mott's relation¹ (assuming a local thermal equilibrium)

$$S_{\alpha\gamma} = \frac{a}{\sigma_{\alpha\gamma}} \left(\frac{\partial \sigma_{\alpha\gamma}}{\partial \epsilon} \right)_{\epsilon_F}, \quad (32)$$

where $a = \pi^2 k_B^2 T / 3e$, ϵ is the electron energy, and ϵ_F is the Fermi energy:

$$S_+ = S_t - a \frac{\beta \beta'}{1 - \beta^2}, \quad S_- = a \frac{\beta'}{1 - \beta^2}, \quad (33)$$

and

$$S_t = \frac{a}{\sigma_t} \left(\frac{\partial \sigma_t}{\partial \epsilon} \right)_{\epsilon_F} \quad (34)$$

is the *reference thermopower* defined in Eq. (25), and $\beta' = (\partial \beta / \partial \epsilon)_{\epsilon_F}$ is the derivative of the asymmetry conductivity coefficient β taken at the Fermi level. Equation (31) is rewritten

$$\Sigma^{ne} = - \frac{a(\beta^I - \beta^{II})(\sigma_t^I \beta'^I - \sigma_t^{II} \beta'^{II})}{\sqrt{eL^I \sigma_t^I [1 - (\beta^I)^2]} + \sqrt{eL^{II} \sigma_t^{II} [1 - (\beta^{II})^2]}}. \quad (35)$$

A. Magnetothermopower corresponding to GMR and NEAMR

In the case of spin-valve structures (i.e., junctions consisting of layers with parallel or antiparallel magnetizations) and considering identical ferromagnetic layers, we have $\beta_s = \beta^I = -\beta^{II}$ and also $\beta'_s = \beta'^I = -\beta'^{II}$:

$$\Sigma_{GMR}^{\uparrow\downarrow} = -2a\sigma_t \left(\frac{\beta'}{\beta} \right) R_{GMR}^{\uparrow\downarrow}. \quad (36)$$

Note that according to Eq. (18), at fixed β , $\Sigma_{GMR}^{\uparrow\downarrow}$ is proportional to l_{sf} . As discussed in Ref. 16, the MTEP associated with GMR vanishes if the parameter β' is zero—i.e., if the conductivity asymmetry is not energy dependent. The proportionality between R_{GMR}/R_0 and $\Sigma_{GMR}^{\uparrow\downarrow}/(\Delta S_t)$ was observed experimentally,^{14,16,19,20} and the proportionality factor $\mathcal{P}_{GMR} = -(2a/S_t)(\beta'/\beta)$ was found to be of the order of 1–10 in the usual experimental conditions.

Besides, the out-of-equilibrium contribution due to the AMR in a normal/ferromagnetic junction is deduced by taking into account the relevant s - d relaxation channels $\beta_{sd}^N = 1$ (Sec. III B) and $\beta_{sd}'^N = 0$:

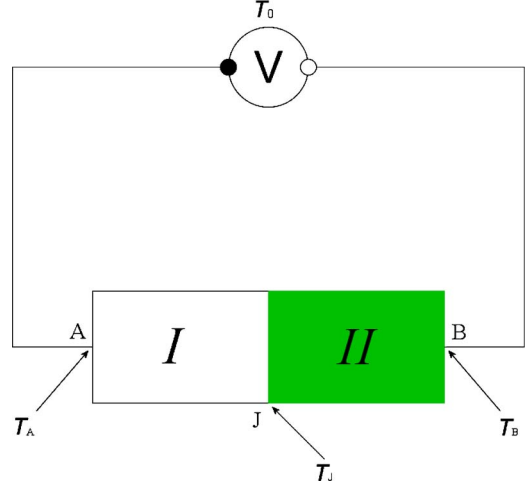


FIG. 2. (Color online) The structure consists of two metallic layers of length AJ and JB with a typical temperature gradient $\Delta T/AB$. It is contacted through two reference wires connected to a voltmeter at temperature T_0 .

$$\Sigma_{AMR}^{N-F} = 2a\sigma^F(\theta) \left(\frac{\beta'(\theta)}{1 - \beta(\theta)} \right) R_{AMR}^{N-F}(\theta). \quad (37)$$

Note that according to Eq. (21), at fixed β , Σ_{AMR}^{N-F} is proportional to l_{diff} . The expression $\Sigma_{AMR}^{ne}/S_t = \mathcal{P}_{AMR}[R_{AMR}^{N-F}/R_0(\theta)]$ [where $R_0(\theta) = \sigma_t(\theta)/\Lambda$] shows that a simple relation similar to that of GMR relates the NEAMR and MTEP. The proportionality factor $\mathcal{P}_{AMR} = (2a/S_t)(\beta'/1 - \beta)$ (refer to AMR/MTEP ratio in the next section) can be measured providing that the NEAMR, described in Sec. III B, Eq. (20), is measured independently (e.g., with the configuration proposed in Refs. 31 and 32). The relevance of the picture proposed above, which is based on the differentiation between two well-separated relaxation channels (spin-flip or s - d scattering), can now be compared to experimental facts.

B. Measuring MTEP

It is important to point out that the measurements of interface TEP necessarily involve the measurement of the TEP of the bulk materials contacted to the voltmeter through reference wires (see Fig. 2). In our experiments, a temperature difference $\Delta T = T_B - T_A$ is maintained between the extremities A and B of the junction (located at the J point), whereas the voltmeter with the terminals of the reference wires are maintained at temperature T_0 . Referring to the TEP of the reference contact as S_r , the total voltage difference measured in the open circuit consists of the bulk TEP and an interface TEP:

$$V_{TEP} = \Delta T \left(\frac{(AJ)S_t^I + (JB)S_t^{II}}{AB} - S_r \right) + \Sigma^{ne} \left(\frac{\partial T}{\partial z} \right)_J. \quad (38)$$

Note that the bulk term appears to be independent of the magnetic configuration (i.e., independent of θ) under the following weakly restrictive condition: $\sigma_t(\epsilon, \theta) = g(\theta)\sigma_t(\epsilon)$ [see Eq. (34)], where $g(\theta)$ is any function accounting for the conductivity anisotropy. In contrast, the out-of-equilibrium term

is still θ dependent through the parameter $\beta(\theta)$ or $l_{sd}(\theta)$. In consequence, we expect that a MTEP contribution can be measured as a function of the external magnetic field and that this MTEP is dominated by the out-of-equilibrium interface effect. On the other hand, the amplitude of the nonequilibrium interface effect depends on the amplitude of the temperature gradient at the junction $(\partial T/\partial z)_j$. The effect is then larger in the case of a nonhomogeneous temperature gradient if the junction is placed in a region where there is a sharp temperature variation—i.e., near the interface with the heat source or cryostat. In contrast, if the junction is placed far away from the interface with the heat source or cryostat, the effect is expected to be smaller.

As for AMR, the θ dependence of the TEP (the MTEP) is defined as the ratio

$$\frac{\Delta V}{V} = \frac{\max\{V(\theta)\} - \min\{V(\theta)\}}{\min\{V(\theta)\}}. \quad (39)$$

In the next section, the quantity $V(\theta)$ is measured as a function of the amplitude and direction of the applied magnetic field \vec{H} .

V. EXPERIMENTS

As already mentioned, the nearly linear relation between the GMR ($\Delta R/R$) and the corresponding MTEP ($\Delta V/V$) has been observed in various spin-valve systems.^{14–20} The GMR/MTEP ratio is of the order of 1–10 in GMR samples consisting of about 150 electrodeposited Co/Cu bilayers where both the GMR and MTEP are of the order of 10%.¹⁹ The present study focuses on MTEP in single Ni nanowires by pointing out the role of the contacts. The results presented hereafter have been measured near room temperature. All nanowires contain two contacts N/F and F/N, and a bulk ferromagnetic (F) region. The results presented in Sec. IV predict that an anisotropic out-of-equilibrium interface magnetoresistance, and corresponding MTEP, should be present at the junctions.

This experimental section is composed as follows. The samples are described in Sec. V A. The magnetic configurations of the nanowire are discussed in Sec. V B on the basis of AMR measurements and of previous studies. Section V C reports on the anisotropic nature of the measured MTEP. Section V D shows that the measured MTEP is an interface effect. Section V E describes the magnetic configurations of the Ni contact that allow the MTEP profiles to be understood.

A. Samples

The samples are prepared by electrodeposition in porous polycarbonate track-etched membranes. This technique has been used extensively in order to study the micromagnetic configurations inside the wires.^{35–41} The pores are $6 \mu\text{m}$ length and 40–25 nm diameter. A gold layer is sputtered on the bottom and top of the membrane and fixed to the electrode. By applying the potential in the electrolytic bath, the Ni nucleates at the bottom of the pores, grows through the membrane, and reaches the top Au layer. Then, a single nanowire can be contacted inside the electrolytic bath by controlling the potential between the two sides of the mem-

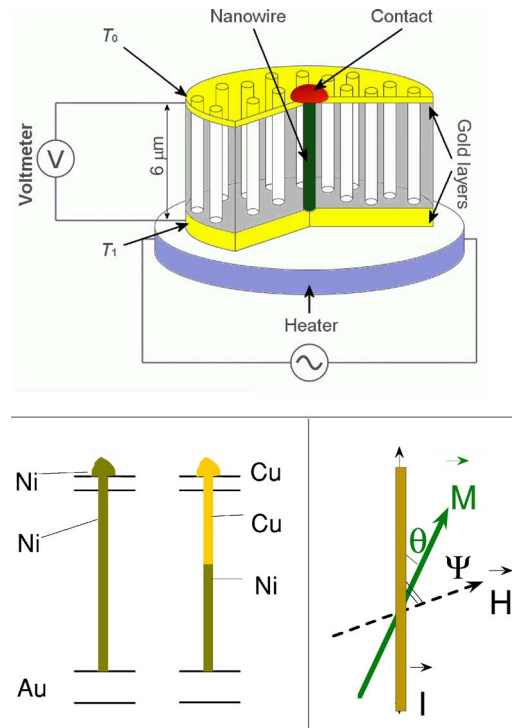


FIG. 3. (Color online) Geometry and contacts of the two kinds of single contacted nanowires. The heat resistance at the bottom is driven by an ac voltage generator at frequency f . T_0 and T_1 are the temperatures of the thermostats.

brane during the electrodeposition and stopping the process when the potential drops to zero.³⁷ By changing the electrolytic bath, the final electric single contact (see Fig. 3) can be performed either with the same material as that of the wire (Ni) or with a different material (for instance, nonferromagnetic like Cu or Au). In the first case the F/N junction coincides with the interface with the top layer (i.e., the heat sink) and in the second case, the F/N junction is located deep inside the wire. The contact (Ni, Cu, or Au) has the shape of a mushroom on top of the membrane.^{37–39}

The electrodeposited Ni nanowire consists of nanometric nanocrystallites with random orientations: the magnetocrystalline anisotropy is averaged out at the nanometer scale.^{23,39–41} Only a strong uniaxial shape anisotropy remains present (anisotropy field $H_a = 2\pi M_s \approx 0.3$ T, where M_s is the magnetization at saturation). It has been shown that the Ni nanowires are uniformly magnetized for all stable states.^{39,40} Furthermore, due to the high aspect ratio, the spatial distribution of the current density \vec{J} is well defined along the wire axis: the angle (\vec{J}, \vec{M}) between the current and magnetization \vec{M} coincides with the angle θ of the magnetization with the wire axis (see Fig. 3).

It is expected that a ferromagnetic contact localized on the top of the membrane (the Ni mushroom) changes the interface properties for two reasons: due to the nonuniform spin-polarized current density⁴² and due to the presence of specific magnetic configurations that do not exist inside the wire. Note that the problem related to the spin accumulation and GMR generated by magnetic domain walls has been studied in detail in such electrodeposited samples.³³ *The con-*

ditions that are necessary to obtain a GMR-like contribution, the presence of a highly constrained magnetic domain wall, are not fulfilled in the present case.⁴³ Here we report on a comparative study between samples with different contacts for a significant number of samples (a few tens). The samples presented in the next subsections are labeled as follows. Sample *A*, Ni wire contacted with Ni (about 38 μV TEP and 3% MTEP); sample *B*, Ni wire contacted with Cu (-4.5 μV TEP and no MTEP); sample *C*, Ni contacted with Ni (-7 μV TEP and no MTEP); sample *D*, Ni contacted with Au (-31.5 μV TEP and no MTEP); sample *E*, Ni contacted with Ni (about -6.4 μV TEP and 3% MTEP). The values are measured for a temperature difference ΔT of about 1 K. Note, however, that the temperature difference is not strictly preserved from one sample to the other because it depends on the details of the heat dissipation at the nanoscopic scales.

B. Magnetic characterization through AMR

Due to the uniform magnetization and to the homogeneous current density, the magnetic field dependence of the AMR is directly linked to the magnetic hysteresis loop of the Ni nanowire. A quadratic dependence is observed:³

$$R(\theta)_0 = R_0 + \Delta R_{AMR} \cos^2(\theta). \quad (40)$$

The magnetoresistance (Fig. 4, sample *A* and sample *B*) is measured with an external magnetic field applied at a given angle Ψ with respect to the wire axis. Except for some few samples where domain walls can be observed (not shown), the hysteresis loop corresponds to a uniform rotation of the magnetization with a precision of two to three percents.^{24,39,40} The magnetic configurations are described by the well-known profile (see, e.g., the Stoner-Wohlfarth model).⁴⁴ At large angles ($\Psi \approx 90^\circ$), the magnetization states follow a reversible rotation from the wire axis $\theta=0$ to nearly the angle of the external field Ψ while increasing the magnetic field from zero to the saturation field (see Fig. 3): intermediate states ($\theta \in [0, 90]$) are stable and correspond to the profile of the AMR curve (Fig. 4). In contrast, for small angles (around $\Psi \approx 10^\circ$) the magnetoresistance profile as a function of the applied field (Fig. 4) is flat because the magnetization is pinned along the wire axis: there are no stable positions between $\theta \approx 10^\circ$ and $\theta \approx 170^\circ$. There is no fundamental change in AMR if the Ni nanowires are contacted with Cu or Au instead of Ni.²⁴

C. MTEP is anisotropic

The thermoelectric measurements are performed with a compact resistive heater (5 Ω), placed at the bottom of the membrane and contacted to a voltage generator of 5–7 V (Fig. 3). A sine wave of frequency of the order of $f = 0.05$ Hz is injected in the heater. At this frequency, a stationary thermal regime is reached and the output thermopower signal is detected at $2f = 0.1$ Hz. The amplitude of the $2f$ signal gives the TEP $\Sigma^{ne} \Delta T / \Lambda$. With our experimental configuration, the amplitude of the TEP ranges between 5 and 50 μV , in agreement with the temperature difference of the order of $\Delta T \approx 1$ K, measured at the macroscopic scale

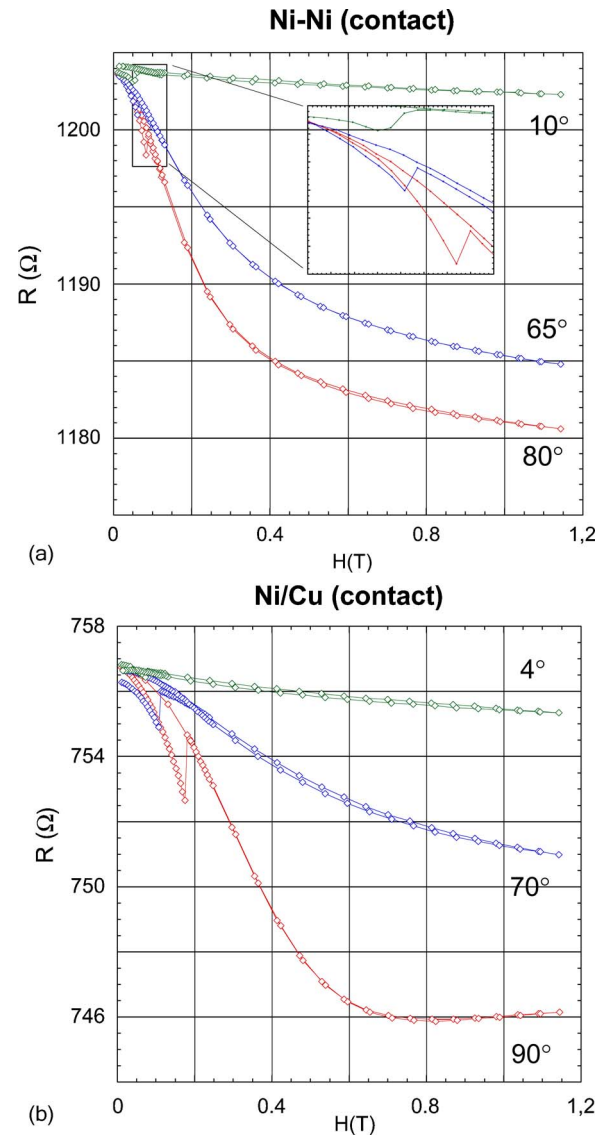


FIG. 4. (Color online) The AMR is plotted at different angles of the external field: (a) Ni wire contacted with Ni (sample *A*) and (b) Ni wire contacted with Cu (sample *B*).

(the bulk values of the Seebeck coefficient are $S_T^{\text{Ni}} \approx -13$ $\mu\text{V}/\text{K}$ and $S_T^{\text{Cu}} \approx 1.8$ $\mu\text{V}/\text{K}$). The temperature gradient is hence $\Delta T / \Lambda \approx 3 \times 10^5$ K/m. These values are close to those measured in electrodeposited Co/Cu/Co multilayered spin valves.^{19,20}

A MTEP signal is obtained by measuring the voltage at zero current, as a function of the applied field. The MTEP signal does not originate directly from the magnetic field, because it is related to ferromagnetic configurations: the *anisotropic nature of the MTEP* is observed in Fig. 5 by measuring the TEP voltage as a function of the angle of the applied saturation field (at saturation field, the magnetization aligns with the field: $\theta = \Psi$). The anisotropic MTEP, with a $\Delta V/V$ variation of about 13% (sample *C*), can be compared to the corresponding AMR [1.3% amplitude, fitted with a $\cos^2(\theta + \epsilon)$ law, where ϵ accounts for the misalignment of the wire inside the membrane³⁹] in Fig. 5. The MTEP profile is not very regular and varies slightly from one sample to the

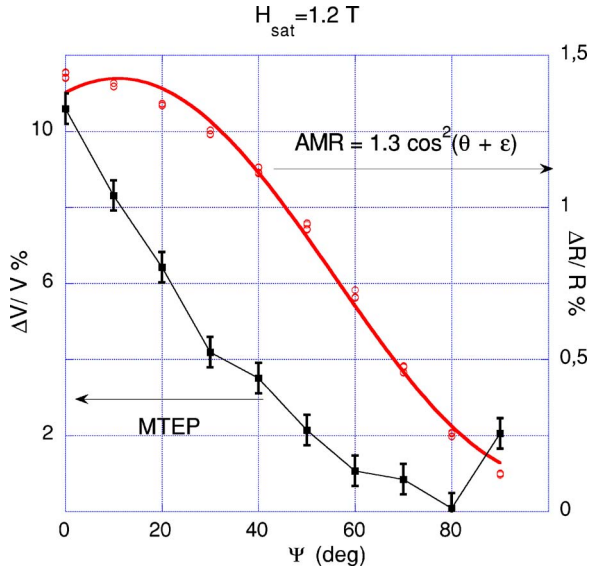


FIG. 5. (Color online) Comparison of magnetothermopower (left) and AMR (right) for a single Ni nanowire with a Ni contact measured as a function of the angle of the external field with a saturating field ($\theta=\Psi$) of 1.2 T (sample C).

other, as can be seen by comparing sample C (Fig. 5) and sample A (Fig. 6 with the points at $H=1$ T for different angles). This variability of the MTEP amplitude from one sample to the other is not surprising since the values of the temperature gradient at the junctions are not controlled at the nanoscopic size in our experiments.

The typical MTEP signal of Ni nanowires contacted with Ni, measured as a function of the external field, is shown in Fig. 6 for sample A characterized in Fig. 4(a). The points are measured with decreasing and increasing external fields (i.e.,

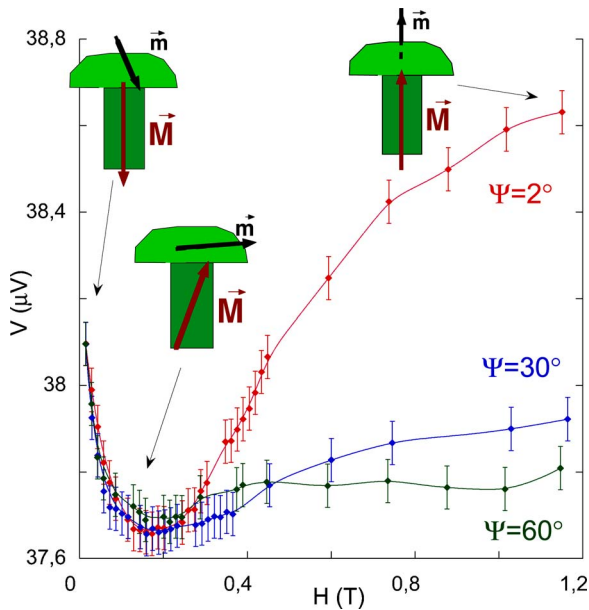


FIG. 6. (Color online) Thermoelectric power as a function of the external field in Ni nanowires contacted with Ni for different directions of the external field. The magnetic configurations of the Ni contact are represented with arrows for $\Psi \approx 2^\circ$ (sample A).

the whole hysteresis loop is measured), but the hysteretic part (observed in the AMR) is not observed. A variation larger than that of the AMR signal is seen (depending on the samples, the MTEP amplitude ranges from about $\Delta V/V = 3\%$ up to 30%) and is of the same order as that of the MTEP produced in GMR devices composed of 150 bilayers.¹⁹ The overall shape is surprising, since the profile as a function of the external field \vec{H}_{ext} at small angles Ψ shows the maximum variation (while the magnetization is fixed along the wire axis), and inversely, the profile at large angle Ψ is approximately flat (while the magnetization rotates from zero to 90°), just the contrary to what is measured with AMR. This typical profile will be analyzed in Sec. V E below. Note that the MTEP minimum at small angles corresponds to the zone of switching field (see Fig. 4) and that the high-field profile shows an approach to saturation corresponding to the anisotropy field of the wire (i.e., in the same range of the applied field). Such curves are systematically observed on all measured samples with small diameters (about 15 samples of diameter about 40 nm).⁴⁵

D. MTEP is not a bulk effect

The MTEP profile is not a function of the angle θ between the magnetization of the Ni nanowire and the wire axis, and the variations observed should be related to another parameter. The most likely hypothesis is that the variations are produced by the magnetization states confined at the interface close to the Ni contact. *In contrast to the AMR which is a bulk effect, the MTEP appears as an interface out-of-equilibrium process.*

This hypothesis can easily be checked by comparing the Ni nanowires contacted with Ni to those contacted with Cu or Au (see Fig. 3). In these last samples, the ferromagnetic/normal interfaces are located inside the nanowire where electric current, temperature gradient, and magnetization are homogeneous. We observe that the MTEP signal vanishes with Cu and Au contacts (the TEP measured as a function of the angles Ψ is constant). The two curves measured as a function of the applied field are compared in Fig. 7 (concerning the samples A and B, characterized in Fig. 4, and D), for $\Psi = 0^\circ$ and $\Psi = 90^\circ$ for samples B and D. These measurements first confirm that the effect is due to the interface and, second, that the role played by the Ni contact is essential for the observation of MTEP processes. Note that a similar role of the Ni contact has been observed in experiments of spin-injection-induced magnetization switching,²⁴ where irreversible magnetization reversal provoked by the current was observed with ferromagnetic contacts, but not with Cu contacts.

These observations corroborate the analysis performed in Sec. IV B where the amplitude of the effect is shown to be proportional to $\Sigma^{ne} \Delta T / AB$. In our experimental configuration, the bottom interface is suspected to play a minor role. It can be suspected that the local temperature gradient at the contact with the Au layer dominates the temperature gradient in the rest of the structure. Near the Ni mushroom at the Ni/Au interface, the ratio $\Delta T / AB$ is large. In contrast, in the case of Cu or Au top contacts, the ferromagnetic/normal junction is located inside the wire where the temperature

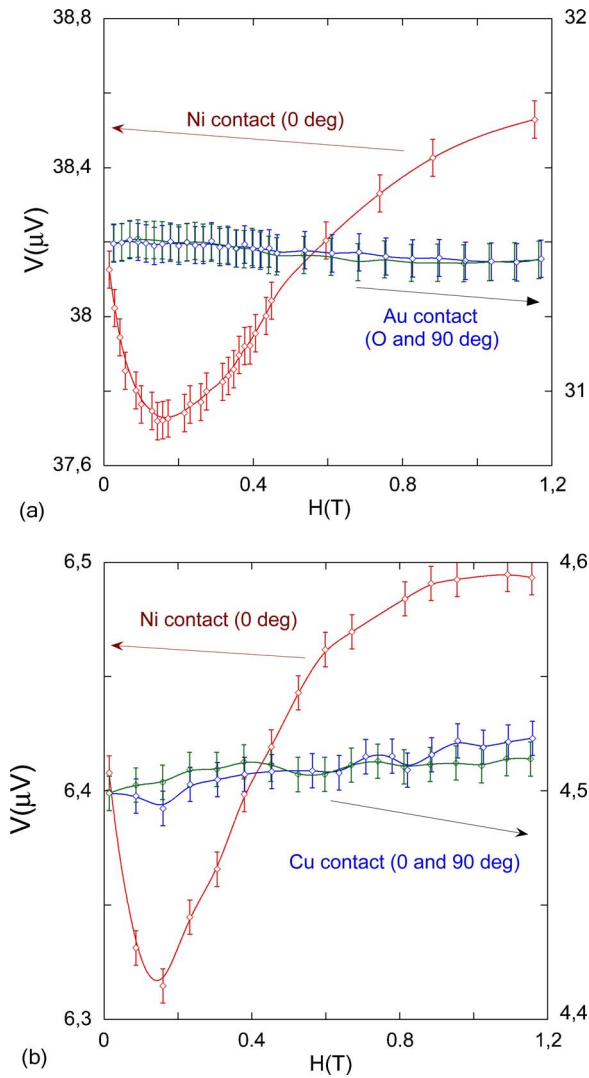


FIG. 7. (Color online) Comparison between magnetothermopower of Ni nanowires contacted with Ni (measured with external field $\Psi \approx 0^\circ$) and Au and Cu contacts ($\Psi \approx 0^\circ$ and $\Psi \approx 90^\circ$) (a) Ni with Ni contacts (sample \mathcal{A} , left scale) compared with Au contact (sample \mathcal{D} , right scale) and (b) Ni with Ni contacts (sample \mathcal{E}) compared with Cu contacts (sample \mathcal{B}).

gradient is expected to be small: the corresponding interface MTEP signal is then small.

E. MTEP is related to the magnetic configurations of the Ni contact

In the previous section, we have shown that the MTEP is an interface effect. The aim of the present section is to show that the MTEP signal observed is generated by the magnetization configurations of the Ni contact on the top of the membrane.

It is indeed possible to relate the observed MTEP to the magnetic configuration if we consider that the relevant angle is the angle $\theta_{NIF} = (\vec{I}_{NIF}, \vec{M}_{NIF})$ between the local current I and the magnetization M at the nanoscopic scale near the N/F interface. With Cu and Au contacts, both the current density

and the magnetization direction are well defined, and the angles coincide with that of the AMR: $\theta_{NIF} = (\vec{I}_{NIF}, \vec{M}_{NIF}) = \theta$. However, with the Ni contact, the interface is located near the Ni mushroom. The magnetic configurations do not follow that measured with AMR inside the wire (see Fig. 6). The MTEP variations can then be reproduced assuming that the magnetization of the mushroom rotates following the total magnetic field $\vec{H}_T = \vec{H}_a + \vec{H} + \vec{H}_{perp}$ where \vec{H}_a is the dipole field due to the wire (which is of the order of the shape anisotropy of the wire) and \vec{H} is the applied field. The field \vec{H}_{perp} is the shape anisotropy of the mushroom. It is produced by the dipole field of the mushroom, probably interacting with the other vicinity mushrooms in the plane of the membrane (it plays the role of the anisotropy field of a thin layer). Thus the cases of large and small angles have to be distinguished: (i) The application of the external field at large angles fixes the magnetization of all mushrooms in the plane perpendicular to the wire axis so that the configuration with the magnetization of the mushroom along the wire axis is expected only near zero applied field where H_a dominates. (ii) In the case of an external magnetic field applied at small angles $\Psi \leq 10^\circ$ (see schemes in Fig. 6), the magnetization of the mushroom is along the wire axis for nearly zero field (H_a dominates) and for saturation fields (H dominates). At intermediate fields, the magnetization of the wire switches to the opposite direction: a domain wall should be present between the wire and mushroom. The transverse field \vec{H}_{perp} dominates. The above scenario describes well the curves observed at different angles: the minima correspond to the MTEP with the magnetization of the mushroom perpendicular to the wire axis. The maximal value of MTEP corresponds to the magnetization of the mushroom parallel to the wire axis.

VI. CONCLUSION

The well-known two-spin-channel model has been extended to the general case of an interface between two layers in the relaxation time approximation. A general expression of the thermoelectric power is derived. Like giant magnetoresistance, a nonequilibrium interface resistance contribution due to the anisotropic magnetoresistance is predicted [Eq. (38)] in a ferromagnetic/normal interface due to s - d interband relaxation. The corresponding magnetothermopower is derived and is found to be proportional to $l_{diff}(\partial T / \partial z)_J$ [Eq. (37)] where l_{diff} is the relevant diffusion length and $(\partial T / \partial z)_J$ is the temperature gradient at the junction (see Fig. 2). The MTEP associated with GMR is proportional to the magnetoresistance with the proportionality coefficient $\mathcal{P}_{GMR} = -(2a/S_t)(\beta'/\beta)$ and the MTEP associated with AMR is proportional to the out-of-equilibrium AMR, with coefficient $\mathcal{P}_{AMR} = (2a/S_t)[\beta'/(1-\beta)]$. In the case of GMR, the experimental value of \mathcal{P}_{GMR} is close to 1 (Ref. 19) (the MTEP is of the same order as the GMR) for many junctions in series.

In complement to the experiments with multilayered systems (Co/Cu/Co),¹⁹ measurements of MTEP in electrodeposited Ni nanowires are presented. This signal shows three striking features: (i) a large MTEP signal of several μV for about 1 K temperature variation is measured (3–30% of the

TEP), (ii) this MTEP is anisotropic, and (iii) the measured MTEP signal is produced by a local magnetic configuration (at nanometric range) near the interface only. However, in contrast to transport experiments in GMR systems where both the magnetoresistance and magnetothermopower are measured, the out-of-equilibrium AMR is not accessible in our two-point measurements in Ni nanowires. Accordingly, the interpretation of anisotropic MTEP due to GMR (where $\text{MTEP} \propto l_{sf} \Delta T / AB$) produced by magnetic inhomogeneities (i.e., domain wall scattering effects) cannot be directly ruled out. But the interpretation of domain wall TEP is not realistic because domain wall scattering is very weak (below 0.1% if any, according to previous studies³³) so that an important anisotropic MTEP could be measured only with a huge proportionality coefficient (≥ 100), which is in contradiction with the known GMR coefficient ($\mathcal{P}_{GMR} \approx 1$ for 150 junctions) measured in GMR structures.

The results of this study hence show that, while GMR and the associated thermopower indicates spin-flip diffusion at the interface, the observed interface anisotropic MTEP should indicate interband *s-d* relaxation associated with ferromagnetism in Ni at the interface (where $\text{MTEP} \propto l_{sd} \Delta T / AB$). The amplitude of the effect suggests that the corresponding *sd* diffusion length is sizable (e.g., of the order of the spin-flip length l_{sf}). Within this framework, further experiments allowing direct measurements of nonequilibrium AMR would probe and clarify the role played by the two kinds of relaxation processes.

ACKNOWLEDGMENT

H.J.D. thanks the Délégation Générale pour l'Armement for support.

-
- ¹N. F. Mott and H. Jones, *Theory of the Properties of Metal and Alloys* (Oxford University Press, New York, 1953).
- ²R. Potter, Phys. Rev. B **10**, 4626 (1974).
- ³T. R. McGuire and R. I. Potter, IEEE Trans. Magn. **11**, 1018 (1975).
- ⁴F. J. Blatt, P. A. Schroeder, C. L. Foiles, and D. Greig, *Thermoelectric Power of Metals* (Plenum, New York, 1976), Chap. 5.
- ⁵J. P. Jan, in *Solid State Physics*, edited by F. Seitz and D. Turnbull (Academic, New York, 1957), Vol. 5, pp. 82–84; K. P. Bjelow, *Erscheinungen in Ferromagnetischen Metallen* (VEB Verlag Technik, Berlin, 1953).
- ⁶M. N. Baibich, J. M. Broto, A. Fert, F. Nguyen Van Dau, F. Petroff, P. Etienne, G. Creuzet, A. Friederich, and J. Chazelas, Phys. Rev. Lett. **61**, 2472 (1988); G. Binasch, P. Grunberg, F. Saurenbach, and W. Zinn, Phys. Rev. B **39**, 4828 (1989).
- ⁷T. Valet and A. Fert, Phys. Rev. B **48**, 7099 (1993).
- ⁸M. Johnson and R. H. Silsbee, Phys. Rev. B **35**, 4959 (1987); **37**, 5312 (1988).
- ⁹P. C. van Son, H. van Kempen, and P. Wyder, Phys. Rev. Lett. **58**, 2271 (1987).
- ¹⁰P. M. Levy, H. E. Camblong, and S. Zhang, J. Appl. Phys. **75**, 7076 (1994).
- ¹¹J.-E. Wegrowe, Phys. Rev. B **62**, 1067 (2000).
- ¹²G. Schmidt, D. Ferrand, L. W. Molenkamp, A. T. Filip, and B. J. van Wees, Phys. Rev. B **62**, R4790 (2000).
- ¹³F. J. Jedema, B. J. van Wees, B. H. Hoving, A. T. Filip, and T. M. Klapwijk, Phys. Rev. B **60**, 16549 (1999).
- ¹⁴J. Sakurai, M. Horie, S. Araki, H. Yamamoto, and T. Shinjo, J. Phys. Soc. Jpn. **60**, 2522 (1991).
- ¹⁵L. Piraux, A. Fert, P. A. Schroeder, R. Laloe, and P. Etienne, J. Magn. Magn. Mater. **110**, L247 (1993).
- ¹⁶J. Schi, S. S. P. Parkin, L. Xing, and M. B. Salamon, J. Appl. Phys. **73**, 5524 (1993).
- ¹⁷J. Shi, K. Pettit, E. Kita, S. S. P. Parkin, R. Nakatani, and M. B. Salamon, Phys. Rev. B **54**, 15273 (1996).
- ¹⁸E. Y. Tsymal, D. G. Pettifor, J. Shi, and M. B. Salamon, Phys. Rev. B **59**, 8371 (1999).
- ¹⁹L. Gravier, J.-E. Wegrowe, T. Wade, A. Fabian, and J.-Ph. Ansermet, IEEE Trans. Magn. **38**, 2700 (2002).
- ²⁰L. Gravier, A. Fabian, A. Rudolf, A. Cachin, J.-E. Wegrowe, and J.-Ph. Ansermet, J. Magn. Magn. Mater. **271**, 153 (2004); L. Gravier, S. Serrano-Guisan, and J.-Ph. Ansermet, J. Appl. Phys. **97**, 10C501 (2005); L. Gravier, S. Serrano-Guisan, F. Reuse, and J.-Ph. Ansermet, Phys. Rev. B **73**, 024419 (2006).
- ²¹L. Berger, J. Appl. Phys. **55**, 1954 (1984); P. P. Freitas and L. Berger, *ibid.* **57**, 1266 (1985).
- ²²J. Grollier, D. Lacour, V. Cros, A. Hamzic, A. Vaures, and A. Fert, J. Appl. Phys. **92**, 4825 (2002).
- ²³D. Kelly, J.-E. Wegrowe, Trong-kha Truong, X. Hoffer, Ph. Guitienne, and J.-Ph. Ansermet, Phys. Rev. B **68**, 134425 (2003).
- ²⁴J.-E. Wegrowe, M. Dubey, T. Wade, H.-J. Drouhin, and M. Konczykowski, J. Appl. Phys. **96**, 4490 (2004).
- ²⁵J.-E. Wegrowe and H.-J. Drouhin, Proc. SPIE **5732**, 498 (2005); cond-mat/0408410 (unpublished).
- ²⁶The case of up- and down-spin electrons is obvious. In the case of *s*- and *d*-channel band hybridization was often invoked against this distinction. However, even when dealing with hybridized states, it is still possible to separate conduction channels with a dominant *s* character from conduction channels originating from states with a stronger *d* contribution.
- ²⁷Motofumi Suzuki and Yasunori Taga, Phys. Rev. B **52**, 361 (1995).
- ²⁸R. J. Baxter, D. G. Pettifor, E. Y. Tsymal, D. Bozec, J. A. D. Matthew, and S. D. Thomson, J. Phys.: Condens. Matter **15**, L695 (2003).
- ²⁹In all these calculations, the channel parameters $\sigma_{\alpha\gamma}$, β , and L are considered as constant in space. It can be shown that taking into account the gradient only introduces vanishingly small corrections.
- ³⁰The Riemann integral is evaluated in the intervals where the derivative is regular. Note that a global calculation over $[A, B]$, within the framework of the distribution theory yields zero because $\Delta\mu(A) = \Delta\mu(B) = 0$. This simply means that the integral of the regular part is opposite to the integral of the Dirac masses located at the interface. Let us write that the out-of-equilibrium resistance is straightforwardly connected to the chemical poten-

tial drop between the A and B points, diminished by the standard potential drop which would result from the application of Ohm's law. We obtain $J_e R^{ne} = [\mu_I(A) - \mu_{II}(B)] - e[\Phi_I(A) - \Phi_I(0^-)] - e[\Phi_{II}(0^+) - \Phi_{II}(B)] = [\mu_I(A) - e\Phi_I(A)] - [\mu(0) - e\Phi_I(0^-)] + [\mu(0) - e\Phi_{II}(0^+)] - [\mu_{II}(B) - e\Phi_{II}(B)] = e[\Phi_I(0^-) - \Phi_{II}(0^+)]$. It can be seen that the second expression for $J_e R^{ne}$ above is nothing but the opposite of Eq. (6) and is equal to the discontinuity of Φ at the interface, which provides a simple physical interpretation as illustrated in Fig. 1.

- ³¹F. J. Jedema, A. T. Filip, and B. J. van Wees, *Nature (London)* **410**, 345 (2001).
³²J.-M. George, A. Fert, and G. Faini, *Phys. Rev. B* **67**, 012410 (2003).
³³J.-E. Wegrowe, A. Comment, Y. Jaccard, J.-Ph. Ansermet, N. M. Dempsey, and J.-Ph. Nozières, *Phys. Rev. B* **61**, 12216 (2000).
³⁴It is clear that the corresponding model should include four channels that take into account the two spin channels for each s and d band. This more involved description is performed elsewhere [see J.-E. Wegrowe and H.-J. Drouhin, cond-mat/0408410 (unpublished)]. For the sake of simplicity, we limit here the discussion to two independent models, with two spin-polarized channels on the one hand and s and d conduction channels on the other hand.

- ³⁵T. L. Wade and J.-E. Wegrowe, *Eur. Phys. J.: Appl. Phys.* **29**, 3 (2005).
³⁶A. Fert and L. Piraux, *J. Magn. Magn. Mater.* **200**, 338 (1999).
³⁷J.-E. Wegrowe, S. E. Gilbert, V. Scarani, D. Kelly, B. Doudin, and J.-Ph. Ansermet, *IEEE Trans. Magn.* **34**, 903 (1998).
³⁸C. Schoenenberger, B. M. I. van der Zande, L. G. J. Fokkink, M. Henny, M. Krueger, A. Bachtold, R. Huber, H. Birk, U. Stauffer, and C. Schmid, *J. Phys. Chem. B* **101**, 5497 (1997).
³⁹Y. Jaccard, P. Guittienne, D. Kelly, J.-E. Wegrowe, and J.-Ph. Ansermet, *Phys. Rev. B* **62**, 1141 (2000).
⁴⁰J.-E. Wegrowe, D. Kelly, A. Franck, S. E. Gilbert, and J.-Ph. Ansermet, *Phys. Rev. Lett.* **82**, 3681 (1999).
⁴¹J. Meier, B. Doudin, and J.-Ph. Ansermet, *J. Appl. Phys.* **79**, 6010 (1996).
⁴²J. Hamrle, T. Kimura, T. Yang, and Y. Otani, *Phys. Rev. B* **71**, 094434 (2005).
⁴³Ch. Marrows, *Adv. Phys.* **54**, 585 (2005).
⁴⁴A. Aharoni, *Introduction to the Theory of Ferromagnetism* (Clarendon, Oxford, 1996).
⁴⁵Some nanowires with very high AMR (about 3%) and large diameter show a MTEP profile as a function of the magnetic field that follows the AMR profile: these samples have a very low contact resistance and no mushroom effects.